Fingerprints of a Bosonic Symmetry-Protected Topological State in a Quantum Point Contact

Rui-Xing Zhang and Chao-Xing Liu
Department of Physics, The Pennsylvania State University, University Park, Pennsylvania 16802, USA
(Received 24 October 2016; published 26 May 2017)

In this work, we study the transport through a quantum point contact for bosonic helical liquid that exists at the edge of a bilayer graphene under a strong magnetic field. We identify "smoking gun" transport signatures to distinguish a bosonic symmetry-protected topological (BSPT) state from a fermionic two-channel quantum spin Hall (QSH) state in this system. In particular, a novel charge-insulator–spin-conductor phase is found for the BSPT state, while either the charge-insulator–spin-insulator or the charge-conductor–spin-conductor phase is expected for the two-channel QSH state. Consequently, a simple transport measurement will reveal the fingerprint of bosonic topological physics in bilayer graphene systems.

DOI: 10.1103/PhysRevLett.118.216803

Introduction.—Ever since the discovery of topological insulators [1–4], intensive research has been focused on understanding the role of symmetry in protecting new topological states, which are known as "symmetry-protected topological (SPT) states" [5,6]. A grand challenge in this field is to understand the role of interaction in SPT states and to realize interacting SPT states in realistic materials. Recently, it was theoretically proposed that interaction has a dramatic effect on topological properties of bilayer graphene under a tilted magnetic field [7]. The strong magnetic field guarantees the spin conservation, and drives the system into a quantum spin Hall (QSH) state with edge states described by fermionic two-channel helical Luttinger liquid. Experimentally [8], the two-terminal conductance is found to approach $4e^2/h$ when chemical potential is tuned into the Zeeman gap between two spin-polarized zeroth Landau levels, which serves as the key signature of helical edge transport in the QSH physics [9–14]. In Ref. [7], we analyze the interaction effect in bilayer graphene and demonstrate that fermionic degrees of freedom on the boundary are generally gapped out. A pair of bosonic edge modes, however, remains gapless as a result of the symmetry protection of charge conservation [$U(1)_c$ symmetry] and spin conservation [$U(1)_s$ symmetry]. Thus, interactions drive the whole system from a two-channel QSH state into a bosonic version of topological insulators, known as the bosonic SPT (BSPT) state [5,6,15–17]. Since a pair of dual boson fields of this bosonic edge mode carry charge-$2e$ excitation and spin-1 excitation, respectively, and preserve the helical nature, we dub them "bosonic helical liquid." Therefore, bilayer graphene under a strong magnetic field provides us a unique opportunity to study interacting topological physics in realistic materials [18,19].

The aim of this work is to explore transport properties of bosonic helical liquid of the BSPT state in bilayer graphene and identify key signatures to distinguish the BSPT state from the fermionic QSH state. First of all, the bosonic charge-$2e$ edge excitation of the BSPT state carries electric currents and a two-terminal measurement will also reveal $4e^2/h$ conductance, taking into account two edges in a realistic sample. Thus, the two-terminal transport measurements [8] *cannot* distinguish the BSPT state from the QSH state in bilayer graphene. Several possible experimental probes, such as shot noise measurement of $2e$ charge, have been considered in Ref. [7]. However, such noise measurement is experimentally challenging and sometimes controversial, and a simple transport detection of the BSPT state is desirable.

In this Letter, we study a quantum point contact (QPC) between two edges of bilayer graphene under a tilted magnetic field, as shown in Fig. 1. With the help of this QPC setup, fingerprints of the BSPT state are clearly revealed in the phase diagram of interedge tunneling physics. Based on the realistic interaction in bilayer graphene, our main results show (1) a novel charge-insulator–spin-conductor phase [20,21], labeled as the IC phase [22], when the BSPT state is formed, and (2) in contrast, either charge-conductor–spin-conductor or charge-insulator–spin-insulator phase, labeled as the CC/II phase, for the fermionic two-channel QSH state, where the BSPT state is not formed. Thanks to the unique transport properties in the IC phase, we propose simple two-terminal conductance measurements in both vertical and horizontal directions in the bilayer graphene QPC. Perfect insulating behaviors in both directions will be the "smoking gun" signal for BSPT physics, unambiguously distinguishing the BSPT state from the fermionic QSH state.

Model Hamiltonian.—We consider a bilayer graphene sample in a four-terminal configuration as shown in Fig. 1. Both in-plane magnetic field ($B_\parallel$) and out-of-plane magnetic field ($B_\perp$) are required to drive the system into the QSH regime with two-channel helical Luttinger liquid on the boundary [8,23]. A strong asymmetric potential (V_A)

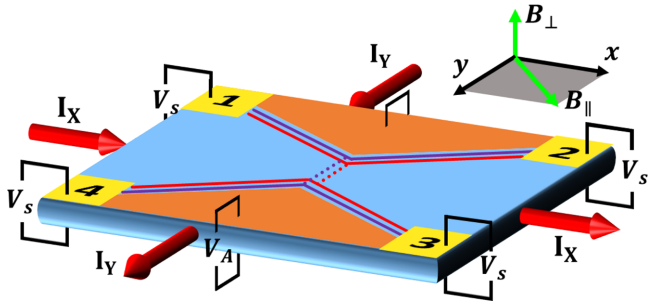

FIG. 1. QPC setup of a bilayer graphene sample is plotted, where a tilted magnetic field is applied. The BSPT regime is colored in blue, while symmetric potential V_S and asymmetric potential V_A are applied to the yellow and orange regime. Here V_S locally shifts the chemical potential to drive the yellow parts of the sample to be metallic, which thus act as leads.

induced by a gate voltage can drive the system into a layer polarized insulating phase with a trivial gap [24–26]. As a result, we can locally gate the sample and nontrivial edge modes exist at the interface between the unbiased region (blue region) and the biased region (orange region), as shown in Fig. 1. The local gates can be designed to form a QPC configuration in this device and the tunneling between two edges only occurs at the QPC.

As justified in the Supplemental Material [27], helical edge modes can exist in both edges and are labeled by the fermionic operators $\psi_{i,l,\lambda}$ that are connected to the lead $i \in \{1,2,3,4\}$ and characterized by a channel index $1 \in \{\mathrm{I},\mathrm{II}\}$ and a direction index $\lambda \in \{\mathrm{in},\mathrm{out}\}$. The Abelian bosonization technique is applied and the corresponding bosonic chiral fields $\chi_{i,l,\lambda}$ are defined as $\psi_{i,l,\lambda} = (F_{i,l,\lambda}/\sqrt{2\pi a_0})e^{if(\lambda)\sqrt{4\pi}\chi_{i,l,\lambda}}$, with the Klein factor $F_{i,l,\lambda}$, the coefficient $f(\lambda) = +1(-1)$ for a right (left) mover and the short-distance cutoff a_0. Let us define the edge that connects the leads 1 (3) and 2 (4) as the top (bottom) edge and the bosonic chiral fields on each edge are related to the $\chi_{i,l,\lambda}$ field by

$$\begin{aligned}\chi_{t(b),l,R} &= \chi_{1(4),l,\mathrm{out}}(-x)\Theta(-x) - \chi_{2(3),l,\mathrm{in}}(x)\Theta(x),\\ \chi_{t(b),l,L} &= \chi_{1(4),l,\mathrm{in}}(-x)\Theta(-x) - \chi_{2(3),l,\mathrm{out}}(x)\Theta(x),\end{aligned} \tag{1}$$

with step function $\Theta(x)$. Here the $+x$ direction is defined along the edge from lead 1 (4) to lead 2 (3). The dual boson fields are introduced as $\phi_{t(b),l} = \chi_{t(b),l,R} + \chi_{t(b),l,L}$ and $\theta_{t(b),l} = -\chi_{t(b),l,R} + \chi_{t(b),l,L}$. Together with the unharmonic terms that respect both $U(1)_c$ and $U(1)_s$ symmetries, the full Hamiltonian is given by

$$\begin{aligned}\mathcal{H} = &\sum_{s\in\{t,b\}}\sum_{l=\pm}\frac{v_l}{2}\left(K_l(\partial_x\phi_{s,l})^2 + \frac{1}{K_l}(\partial_x\theta_{s,l})^2\right)\\ &+ g_1\sum_s \cos 2\sqrt{2\pi}\phi_{s,-} + g_2\sum_s \cos 2\sqrt{2\pi}\theta_{s,-},\end{aligned} \tag{2}$$

where $\phi_{s,\pm} = (1/\sqrt{2})(\phi_{s,\mathrm{I}} \pm \phi_{s,\mathrm{II}})$ and $\theta_{s,\pm} = (1/\sqrt{2})(\theta_{s,\mathrm{I}} \pm \theta_{s,\mathrm{II}})$ are bonding and antibonding fields, respectively. When $g_1 = g_2 = 0$, this Hamiltonian describes the low-energy edge physics of the QSH state with a spin Chern number 2. Here $K_\pm = \sqrt{(2\pi v_f + 2g_5 + g_3 \pm g_4)/(2\pi v_f + 2g_5 - g_3 \mp g_4)}$, and it is expected that $K_- > 1$. An explicit definition of g_3 and g_4 can be found in the Supplemental Material [27]. A nonzero g_1 term is relevant, which will freeze the $\phi_{s,-}$ field as $\phi_{s,-} = [(2n_s+1)\pi]/2\sqrt{2\pi}$ with $n_s \in \mathbb{Z}$, and gap out the antibonding boson modes. The pinning of the $\phi_{s,-}$ field is dubbed the "BSPT condition," which mathematically distinguishes bosonic helical liquid from two-channel helical Luttinger liquid. We further introduce the notation of the spin-charge basis as

$$\phi_\rho = \phi_{+,+}, \quad \phi_\sigma = \theta_{-,+}, \quad \theta_\rho = \theta_{+,+}, \quad \theta_\sigma = \phi_{-,+}, \tag{3}$$

with $\phi_{s=\pm,+} = (\phi_{t,+} \pm \phi_{b,+})/\sqrt{2}$ and $\theta_{s=\pm,+} = (\theta_{t,+} \pm \theta_{b,+})/\sqrt{2}$. The corresponding Hamiltonian is

$$\mathcal{H}_{\mathrm{BSPT}} = \sum_{r=\rho,\sigma}\frac{v_+}{2}\left(K_+(\partial_x\phi_r)^2 + \frac{1}{K_+}(\partial_x\theta_r)^2\right). \tag{4}$$

Therefore, the remaining free bosonic bonding fields $\phi_{s,+}$ and $\theta_{s,+}$ form helical bosonic edge modes carrying spin 1 and charge $2e$.

Tunneling physics and phase diagram.—For the QPC structure, the tunneling process is expected to take place at the contact point $x = 0$. Interedge tunnelings for a QSH state are only constrained by the symmetries of the system. In a BSPT QPC setup, however, tunneling terms are additionally constrained by the BSPT condition defined above. We will show that this requirement not only constrains the explicit form of the tunneling process, but also modifies the scaling dimension of tunneling operators and greatly changes the phase diagram of the tunneling process.

Let us start with the single-particle tunneling, and $U(1)_s$ symmetry requires that an electron must switch its velocity when hopping between different edges. Generally, the single-particle tunneling operator is

$$T_{l,l'} = t_{l,l'}\psi^\dagger_{t,l,L}\psi_{b,l',R} + \mathrm{H.c.} \tag{5}$$

In the bosonized language, $T_{l,l'} = t_{l,l'}\cos\sqrt{\pi}[\phi_{+,+} + \theta_{-,+} - f_+(\phi_{+,-} + \theta_{-,-}) - f_-(\phi_{-,-} + \theta_{+,-})]$, where $f_\pm = \frac{1}{2}[(-1)^l \pm (-1)^{l'}]$. The BSPT condition guarantees that the correlation function of its dual fields $\langle\theta_{s,-}(\tau)\theta_{s,-}(0)\rangle$ diverges as $g_1 \to \infty$ [27]. As a result, the correlation function of any vertex operator of $\theta_{s,-}$ vanishes since $\langle e^{i\alpha\theta_{s,-}(\tau)}e^{-i\alpha\theta_{s,-}(0))}\rangle = e^{[-(\alpha^2/2)]\langle[(\theta_{s,-}(\tau)-\theta_{s,-}(0))^2]\rangle}$. This immediately implies that any vertex operator of $\theta_{s,-}$ is vanishing under RG operation. Since $\theta_{s,-}$ always appears in $T_{l,l'}$, we conclude that

single particle tunneling $T_{l,l'}$ is generally forbidden in the BSPT QPC. Physically, this implies that single-particle tunneling is incompatible with the BSPT condition, and violates the bosonic nature of the BSPT state.

Next, we examine the two-particle tunneling shown in Fig. 2(a), where a right mover on the top edge (spin-up) tunnels to a left mover on the bottom edge (spin-up), and a right mover on the bottom edge (spin-down) simultaneously tunnels to a left mover on the top edge (spin-down). As a result, the charge transfer between the top and bottom edges is zero, while the spin transfer is one. This type of spin-1 tunneling process is mathematically described by

$$V^{\sigma} = v^{\sigma}_{l_1,l_2,l_3,l_4}\psi^{\dagger}_{b,L,l_1}\psi_{t,R,l_2}\psi^{\dagger}_{t,L,l_3}\psi_{b,R,l_4} + \text{H.c.}, \quad (6)$$

where $l_{1,2,3,4} \in \text{I}, \text{II}$. Under the BSPT condition, the absence of the antibonding field $\theta_{s,-}$ in V^{σ} yields a strong constraint on the channel index l_i: $l_1 = l_4 = l, l_2 = l_3 = l'$, which leads to

$$V^{\sigma} = v^{\sigma}\cos 2\sqrt{\pi}\phi_{+,+} = v^{\sigma}\cos 2\sqrt{\pi}\phi_{\rho}. \quad (7)$$

There exists another type of symmetry allowed two-particle tunneling term, which describes the interedge transfer of the $2e$ charge and zero spin, as shown in Fig. 2(b):

$$V^{\rho} = v^{\rho}_{l_1,l_2,l_3,l_4}\psi^{\dagger}_{b,L,l_1}\psi_{t,R,l_2}\psi^{\dagger}_{b,R,l_4}\psi_{t,L,l_3} + \text{H.c.} \quad (8)$$

The condition for a nonvanishing V^{ρ} can be similarly identified as $l_1 \neq l_4$, $l_2 \neq l_3$, leading to the following bosonized expression of charge-$2e$ tunneling as

$$V^{\rho} = v^{\rho}\cos 2\sqrt{\pi}\theta_{-,+} = v^{\rho}\cos 2\sqrt{\pi}\phi_{\sigma}. \quad (9)$$

As shown in Ref. [7], the elementary bosonic excitations on the edge s are found to be either charge-$2e$ spin-singlet Cooper pair $\Phi_{s,q=2e} = \psi_{s,\text{I},R}\psi_{s,\text{II},L} - \psi_{s,\text{I},L}\psi_{s,\text{II},R} \sim e^{-i\sqrt{2\pi}\theta_{s,+}}$ or spin-1 chargeless spinon $\Phi_{s,\sigma=1} = \psi^{\dagger}_{s,\text{I},\downarrow}\psi_{s,\text{I},\uparrow} - \psi^{\dagger}_{s,\text{II},\downarrow}\psi_{s,\text{II},\uparrow} \sim e^{-i(-1)^s\sqrt{2\pi}\phi_{s,+}}$. For the definition of the bosonic operator $\Phi_{s,\sigma=1}$, we have used the convention $(-1)^t = -1$ and $(-1)^b = 1$, which originates from opposite spin-momentum locking at different edges. The above two-particle tunneling terms can be rewritten as

$$V^{\sigma} = v^{\sigma}\Phi^{\dagger}_{b,\sigma=1}\Phi_{t,\sigma=1} + \text{H.c.},$$
$$V^{\rho} = v^{\rho}\Phi^{\dagger}_{b,q=2e}\Phi_{t,q=2e} + \text{H.c.} \quad (10)$$

Therefore, two-particle tunneling V_{σ} and V_{ρ} are physically interpreted as the tunneling of bosonic quasiparticles across the QPC, as shown in Figs. 2(c) and 2(d). In other words, Eq. (10) demonstrates the minimal tunneling events allowed in a *bosonic* SPT system.

Now we are ready to analyze and compare the phase diagram of tunneling physics for the bilayer graphene QPC structure with and without the formation of the BSPT state. In a series of pioneering works, the QPC physics of fermionic one-channel helical Luttinger liquid and fermionic four-channel helical Luttinger liquid have been studied in a QSH system [20,21,32] and a bilayer graphene with domain walls [33]. The phase diagram of our bilayer graphene QSH state follows the paradigm in the above systems: (1) In the weak interaction limit, both single-particle and two-particle tunneling terms are small and irrelevant, which defines the CC phase. However, a duality transformation of the CC phase reveals another stable fixed point where the QPC is pinched off, giving rise to the so-called II phase [21]. Therefore, CC and II fixed points are separated by a QPC pinch-off transition in this parameter regime. (2) As the repulsive (attractive) interaction strengths exceed critical values, QPC is driven into the IC (CI or charge-conductor–spin-insulator) phase where spin-1 (charge-$2e$) tunneling is relevant. We have mapped out the phase diagram of the fermionic two-channel QSH state in the QPC setup of bilayer graphene, as shown in Fig. 3(a). More details can be found in the Supplemental Material [27].

When the bulk BSPT state is formed, however, the BSPT condition freezes the antibonding degree of freedom and removes the role of K_- in the phase diagram. Scaling dimensions of two-particle tunneling terms are further modified to $\Delta(v^{\sigma}) = (1/K_+)$ and $\Delta(v^{\sigma}) = K_+$, in comparison to the QSH case [27]. This change of scaling dimensions leads to different RG equations

$$\frac{dv^{\sigma}}{da} = \left(1 - \frac{1}{K_+}\right)v^{\sigma}, \qquad \frac{dv^{\rho}}{da} = (1 - K_+)v^{\rho}, \quad (11)$$

with the real space scaling factor a for $v^{\sigma,\rho}$. For $K_+ > 1$, we find v^{σ} is relevant while v^{ρ} is irrelevant, leading to the IC phase. In contrast, the CI phase appears for $K_+ < 1$ and is separated from the IC phase by a critical point at $K_+ = 1$, as shown in Fig. 3(b). Comparing Figs. 3(a) and 3(b), we find two phase diagrams are completely different in the

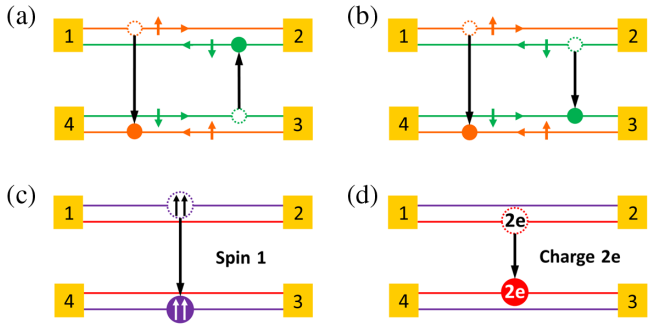

FIG. 2. Two-particle tunneling processes of spin-1 tunneling and charge-$2e$ tunneling are plotted: (i) (a) and (b) in the fermion limit; (ii) (c) and (d) in the BSPT limit.

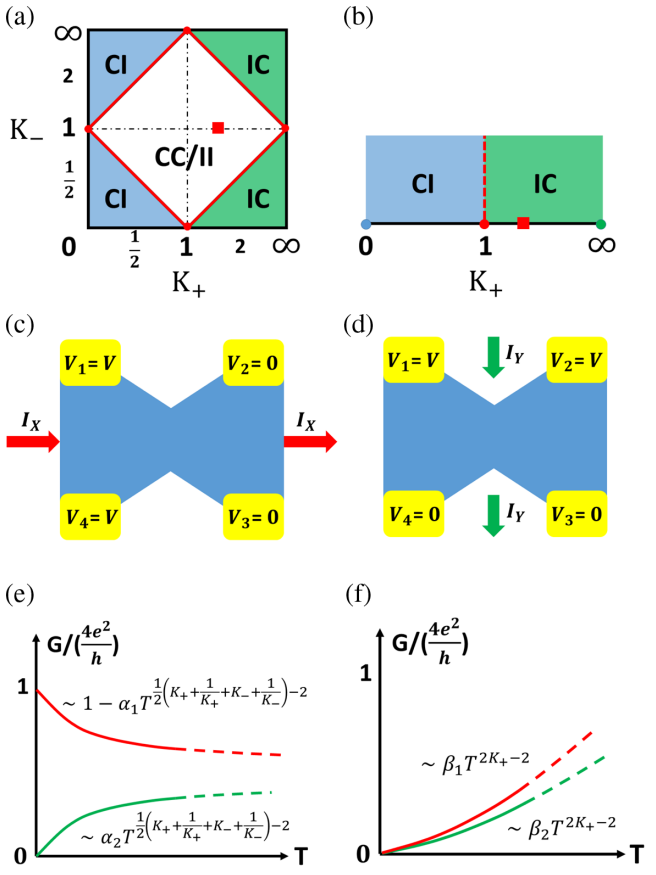

FIG. 3. The phase diagram of the QPC physics is plotted for (i) the two-channel QSH state in (a); (ii) the BSPT state in (b). Voltage configurations of the proposed two-terminal measurement are shown in (c) and (d). The temperature dependence of G_{XX} (red line) and G_{YY} (green line) are also plotted for the QSH state in (e) and the BSPT state in (f).

weak interaction limit $K_+ \approx 1$, thus providing a route to distinguish the BSPT state and the fermionic two-channel QSH state in bilayer graphene.

Experimental detection.—Based on the phase diagram [Figs. 3(a) and 3(b)], we next turn to realistic bilayer graphene systems. First, we need to give an estimate of the Luttinger parameters $K_\pm$, which can be extracted from the screened Coulomb interaction between two edge state electrons. As discussed in the Supplemental Material [27], after mapping the screened Coulomb interaction into the four-fermion interactions in Luttinger liquids, we find that K_+ is determined by the ratio between interaction strength and kinetic energy of the edge modes, while K_- is related to the difference between intra- and inter-Landau level interactions. Assuming the out-of-plane magnetic field to be 2 Tesla and a substrate dielectric constant $\epsilon = 5$, we find that $K_+ = 1.43$ and $K_- = 1.02$ [34] in our bilayer graphene system, which is depicted by the red square in both Figs. 3(a) and 3(b). Based on this estimate, we conclude that the formation of the BSPT state drives the QPC system in bilayer grahene from the CC/II phase into the IC phase. In other words, probing the IC phase in the QPC can serve as the transport evidence of the BSPT state in bilayer graphene.

In the following, we demonstrate that a simple transport measurement will unambiguously distinguish the IC phase from the CC/II phase. We consider applying either horizontal ($V_X = V_1 - V_2 - V_3 + V_4$) or vertical bias voltages ($V_Y = V_1 + V_2 - V_3 - V_4$). The simplest voltage configurations are shown in Figs. 3(c) and 3(d), which are effectively two-terminal setups in two orthogonal directions. A horizontal current $I_X = I_1 - I_2 - I_3 + I_4$ and a vertical current $I_Y = I_1 + I_2 - I_3 - I_4$ can be measured to extract conductances along both directions, where I_i (V_i) is the lead current (voltage) for lead $i \in \{1, 2, 3, 4\}$. The current operators above are related to the boson current operators as $I_X = I_\rho$ and $I_Y + I_\sigma = (4e^2/h)V_Y$. These relations can be easily verified with the help of Eq. (1), together with the definition of spin or charge current $I_{\rho/\sigma} = [-(2\sqrt{\pi})]\partial_t \phi_{\rho/\sigma}$. For the CC phase of the QSH state, both single-particle tunneling and two-particle tunneling terms are irrelevant, so ϕ_ρ and ϕ_σ are free boson fields whose currents are accompanied by a quantized conductance. This gives rise to $I_X = (4e^2/h)V_X$ while $I_Y = 0$. From the duality relation between CC and II phases, we immediately find that $I_Y = (4e^2/h)V_Y$ and $I_X = 0$ for the II phase. Therefore, a QSH sample is always found to be a perfect conductor along either the horizontal or the vertical direction, while it is a perfect insulator along the corresponding orthogonal direction. On the other hand, for a BSPT system, the IC phase exhibits relevant spin-1 tunneling process V^σ, which gaps out only ϕ_ρ field. As a consequence, both I_X and I_Y are vanishing and the current flows in the leads are constrained by $I_1 = -I_2 = I_3 = -I_4$ [20,21]. Thus, the BSPT QPC setup shows the perfect insulating behaviors in both horizontal and vertical directions. This simple and feasible transport measurement will be the smoking gun evidence of the BSPT state.

The distinction between the QSH state and the BSPT state is further demonstrated when temperature effects are incorporated. Temperature dependence of horizontal conductance G_{XX} (red line) and vertical conductance G_{YY} (green line) are plotted in both the CC phase of the QSH state (assuming the CC phase for the QSH state) and the IC phase of the BSPT state. In the CC phase of the QSH state, G_{XX} (G_{YY}) experiences a power-law decay (increase) from the plateau value (zero), and the power-law scaling relation reflects the scaling dimension of single-particle tunneling operators [27]. In the IC phase of the BSPT state, however, both conductances share a similar power-law increase from zero. In contrast to the CC phase, the power of temperature dependence is determined by two-particle (bosonic-particle) tunneling, which only depends on K_+. With our previous estimation of K_+ and K_-, we find $\Delta G_{XX/YY} \sim T^{0.07}$ for the QSH state while $\Delta G_{XX/YY} \sim T^{0.86}$ for the

BSPT state. Therefore, the temperature scaling of G_{XX} and G_{YY} reflects the tunneling mechanism in the QPC for either the QSH state or the BSPT state.

Conclusion.—We proposed that a simple QPC setup "magically" implements two-terminal transport measurements to unambiguously distinguish the BSPT state from the QSH state. In particular, the QPC reveals the fingerprints of bosonic physics in the phase diagram of interedge tunneling physics, and binds the BSPT state with exotic IC physics in the bilayer graphene systems. We notice that the IC phase has not been experimentally realized, probably because it requires a strong interaction in conventional QSH systems. In contrast, our estimate shows that it can be driven by a realistic Coulomb interaction in the bilayer graphene. Another great advantage of bilayer graphene is that its QPC can be feasibly designed and controlled by gate voltages, as shown in Fig. 1, which is absent in other QSH systems. In the Supplemental Material [27], a detailed calculation of the extracting effective charge from the shot noise spectrum is also presented. A bosonic $2e$ charge is found, which originates from the instanton tunneling events of the IC fixed point. Compared with this direct probe of bosonic electric charge, the transport measurements we proposed are much simpler and more feasible for experiment realization.

We would like to thank Cenke Xu for useful discussions. C.-X. L. acknowledges the support from the Office of Naval Research (Grant No. N00014-15-1-2675).

[1] L. Fu, C. L. Kane, and E. J. Mele, Phys. Rev. Lett. **98**, 106803 (2007).
[2] H. Zhang, C.-X. Liu, X.-L. Qi, X. Dai, Z. Fang, and S.-C. Zhang, Nat. Phys. **5**, 438 (2009).
[3] M. Z. Hasan and C. L. Kane, Rev. Mod. Phys. **82**, 3045 (2010).
[4] X.-L. Qi and S.-C. Zhang, Rev. Mod. Phys. **83**, 1057 (2011).
[5] X. Chen, Z.-C. Gu, Z.-X. Liu, and X.-G. Wen, Science **338**, 1604 (2012).
[6] X. Chen, Z.-C. Gu, Z.-X. Liu, and X.-G. Wen, Phys. Rev. B **87**, 155114 (2013).
[7] Z. Bi, R. Zhang, Y.-Z. You, A. Young, L. Balents, C.-X. Liu, and C. Xu, Phys. Rev. Lett. **118**, 126801 (2017).
[8] P. Maher, C. R. Dean, A. F. Young, T. Taniguchi, K. Watanabe, K. L. Shepard, J. Hone, and P. Kim, Nat. Phys. 2013) 154 ,**9**).
[9] C. L. Kane and E. J. Mele, Phys. Rev. Lett. **95**, 226801 (2005).
[10] C. L. Kane and E. J. Mele, Phys. Rev. Lett. **95**, 146802 (2005).
[11] B. A. Bernevig, T. L. Hughes, and S.-C. Zhang, Science **314**, 1757 (2006).
[12] M. König, S. Wiedmann, C. Brüne, A. Roth, H. Buhmann, L. W. Molenkamp, X.-L. Qi, and S.-C. Zhang, Science **318**, 766 (2007).
[13] C. Liu, T. L. Hughes, X.-L. Qi, K. Wang, and S.-C. Zhang, Phys. Rev. Lett. **100**, 236601 (2008).
[14] I. Knez, R.-R. Du, and G. Sullivan, Phys. Rev. Lett. **107**, 136603 (2011).
[15] Y.-Y. He, H.-Q. Wu, Y.-Z. You, C. Xu, Z. Y. Meng, and Z.-Y. Lu, Phys. Rev. B **93**, 115150 (2016).
[16] Y.-Z. You, Z. Bi, D. Mao, and C. Xu, Phys. Rev. B **93**, 125101 (2016).
[17] T. Yoshida and N. Kawakami, Phys. Rev. B **94**, 085149 (2016).
[18] V. Mazo, C.-W. Huang, E. Shimshoni, S. T. Carr, and H. A. Fertig, Phys. Rev. B **89**, 121411 (2014).
[19] V. Mazo, E. Shimshoni, C.-W. Huang, S. T. Carr, and H. Fertig, Phys. Scr. **T165**, 014019 (2015).
[20] C.-Y. Hou, E.-A. Kim, and C. Chamon, Phys. Rev. Lett. **102**, 076602 (2009).
[21] J. C. Y. Teo and C. L. Kane, Phys. Rev. B **79**, 235321 (2009).
[22] Just to clarify, when we talk about the BSPT state or the fermionic QSH state, we refer to the intrinsic bulk topological state of the system, which is independent of the appearance or absence of QPC structure. When we talk about II/IC/CI/CC phases, we refer to the interedge tunneling phase which emerges only when QPC is present.
[23] A. F. Young, J. Sanchez-Yamagishi, B. Hunt, S. H. Choi, K. Watanabe, T. Taniguchi, R. Ashoori, and P. Jarillo-Herrero, Nature (London) **505**, 528 (2014).
[24] E. McCann, Phys. Rev. B **74**, 161403 (2006).
[25] E. V. Castro, K. S. Novoselov, S. V. Morozov, N. M. R. Peres, J. M. B. Lopes dos Santos, J. Nilsson, F. Guinea, A. K. Geim, and A. H. Castro Neto, Phys. Rev. Lett. **99**, 216802 (2007).
[26] M. Kharitonov, Phys. Rev. Lett. **109**, 046803 (2012).
[27] See Supplemental Material at http://link.aps.org/supplemental/10.1103/PhysRevLett.118.216803, which includes Refs. [28–31], for a detailed derivation of Landau levels in bilayer graphene, an estimate of Coulomb interaction and Luttinger parameter, a derivation of Correlation function, a discussion of tunneling phase diagram, and a derivation of effective charges of instanton tunneling and noise spectrum.
[28] E. McCann and M. Koshino, Rep. Prog. Phys. **76**, 056503 (2013).
[29] C. L. Kane and M. P. A. Fisher, Phys. Rev. B **46**, 15233 (1992).
[30] T. Martin, arXiv:cond-mat/0501208.
[31] J. Maciejko, C. Liu, Y. Oreg, X.-L. Qi, C. Wu, and S.-C. Zhang, Phys. Rev. Lett. **102**, 256803 (2009).
[32] A. Ström and H. Johannesson, Phys. Rev. Lett. **102**, 096806 (2009).
[33] B. J. Wieder, F. Zhang, and C. L. Kane, Phys. Rev. B **92**, 085425 (2015).
[34] In our work, the Luttinger parameter $K_{\pm}$ is defined as the inverse of the Luttinger parameter g defined in Ref. [21].